Journal of Wood Science

ORIGINAL ARTICLE

Open Access

Evaluation of increase in loss tangent from longitudinal vibration of wood log by considering apparent density difference between sapwood and heartwood caused by moisture content

Toshiyuki Fukui[1,2*], Yoshiyuki Yanase[1] and Yoshihisa Fujii[3]

Abstract

This study confirmed that the loss tangent (or tangent loss, tan δ) obtained from the longitudinal vibration of a wood log increases with the apparent density difference between sapwood and heartwood, owing to moisture content difference. The reason for this was estimated to be the shear stress occurring when the longitudinal vibration is excited from the calculation of the longitudinal vibration equation for a cylindrical model with different sapwood and heartwood densities. According to the measurement of the vibrational properties of 35 sugi (*Cryptomeria japonica*) logs with large moisture content variation in the sapwood and heartwood, the tan δ for longitudinal vibration increased compared with that for flexural vibration when the apparent sapwood density exceeded apparent heartwood density, whereas the difference in the specific dynamic Young's modulus (E/ρ) was small. To discover why tan δ increases, both the axial and shear strain energy were calculated from the numerical solution of the longitudinal vibration of a cylindrical model by only considering the apparent density difference between sapwood and heartwood. It was found that the shear strain energy increases with the apparent density difference. Because it is known from previous studies that tan δ from the shear strain (tan δ_S) is larger than that from the axial strain (tan δ_A), this study concluded that tan δ increases with the apparent density difference. The ratio of increase of tan δ calculated by the model adequately explaange of the measured tan δ caused by the longitudinal vibration of a sugi log.

Keywords Green wood, Log, Longitudinal vibration, Loss tangent, Moisture content

Introduction

Various useful information, such as the density, strength, and moisture content, can be obtained from logs through non-destructive testing. This enables the detailed arrangement of the drying schedule and the estimation of the air-dried density before processing the logs, leading to efficient log classification. As non-destructive testing methods, previous studies have used X-ray or gamma ray penetration [1, 2], the measurement of speed and attenuation of sound and ultrasound [3, 4], and the resonance frequency from impact vibration, such as flexural vibration by lateral striking or longitudinal vibration by cross-sectional striking [5–7]. Particularly, the impact vibration method has the advantage of simplicity and provides an average value of the entire material. Therefore, this method has been used in previous studies to compare the Young's modulus of logs and timber processed from logs

*Correspondence:
Toshiyuki Fukui
fukui.toshiyuki.34w@st.kyoto-u.ac.jp
[1] Graduate School of Agriculture, Kyoto University, Kyoto, Japan
[2] Daiken Corporation, Osaka, Japan
[3] Kyoto University, Kyoto, Japan

[5, 7]. Additionally, because the moisture content varies extensively from one log to another in some species, the authors developed a density-independent log moisture content estimation method using the specific dynamic Young's modulus (E/ρ) and loss tangent (tan δ) obtained from the flexural vibration of a log [8, 9].

However, when the impact vibration method is used for materials whose properties and moisture contents are not uniform, such as logs, the measured vibrational properties, such as the resonance frequencies, E/ρ, and tan δ, may change owing to the different points of striking or measuring, or different vibration modes. Considering the inhomogeneity of logs, the difference in the moisture content between sapwood, which is responsible for conducting water, and heartwood, which is responsible for supporting the tree body with dead cells, and the resulting apparent density difference, are much larger than the variations in the mechanical properties and oven-dry density in logs. As is well known, the apparent sapwood density can be more than twice that of heartwood [10, 11]. Therefore, it must be clarified whether and why the measured value of the vibrational properties is affected by the apparent density difference between sapwood and heartwood under longitudinal or flexural vibration to improve the accuracy of log evaluation when using these measured values.

However, the influence of the apparent density difference on the vibrational properties, particularly tan δ, for the flexural and longitudinal vibration of logs has not been accurately and quantitatively investigated to date.

This study measured E/ρ and tan δ by the flexural vibration and longitudinal vibration of 35 sugi (*Cryptomeria japonica*) logs, whose heartwood moisture content is known to vary largely from one log to another [10, 11], and investigated the effect of apparent density differences on the longitudinal vibrational properties. It was found that the shear strain energy increases with the apparent density difference. Then, based on previous studies on other materials, such as metals [12–17], the longitudinal vibration equation for a cylindrical model with density differences between sapwood and heartwood was solved to calculate the axial and shear strain energy arising within the model. Subsequently, by combining the calculated axial and shear strain energy and estimating the shear to axial tan δ ratio based on previous studies, this study calculated the amount by which tan δ may change in the presence of density differences. Finally, the calculated tan δ was compared to the measured value.

Materials and methods

Preparation of log specimens

In this study, 35 sugi (*Cryptomeria japonica*) logs purchased at a market in Kyoto were used as specimens. The same specimens used in a previous study by the authors [9] were used, excluding specimens with compression wood or heart shake. The diameter range of all logs at the top end was 200−300 mm, and each log had a length of approximately 4 m. The ratio of the heartwood diameter, including the transition zone, to the log diameter was 0.61−0.81 (average of 0.68), and the ratio of the log length to the average log diameter was 30.8 − 37.2 (average of 33.4).

Vibrational test of log specimens

The configuration of the longitudinal vibration test for the log specimen is shown in Fig. 1. Vibrational tests on the logs were conducted outdoors at 10–20 °C and 30–60% Relative humidity at Kitashirakawa Experimental Station of Kyoto University in Kyoto, Japan. For the longitudinal vibration, the logs were supported at the center using two wooden blocks with a width of 45 mm placed close to each other, with a spacing of approximately 20 mm. A TEAC 701 piezoelectric acceleration sensor (frequency range: 3–30,000 Hz; weight: 3.04 g; TEAC, Tokyo, Japan) was attached to the bottom end cross section, and vibration was excited by striking the top end cross section with a plastic hammer (Fig. 1). The sensor signal was subjected to threefold amplification using an amplifier (TEAC SA-611), and high-pass filtering at 100 Hz or A-weight filtering using a Fast Fourier transform analyzer (Ono Sokki CF5220 or CF9400) to eliminate the low frequency domain. The logarithmic decrement λ was obtained from the waveform during the first 0.4 s after impact. The resonance frequency f_r was obtained in 2.5-Hz increments from the frequency spectrum, which was processed using a Hanning window. From the resonance frequency f_r, logarithmic decrement λ, and dimension of logs, E/ρ and tan δ were calculated. It is noted that in this study ρ denotes density (unit: kg/m^3). For the flexural vibration, the same tests as those in a previous study by the authors [9] were conducted. For the primary mode of flexural vibration, the logs were supported at two

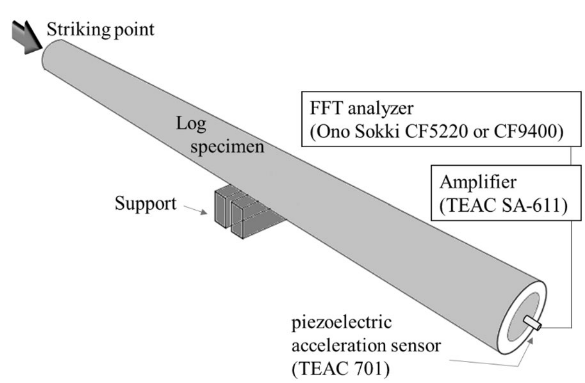

Fig. 1 Configuration of longitudinal vibration test

nodal positions by extruded polystyrene foam (thickness: 30 mm; width: 150 mm; Dupont Styrofoam) on wooden blocks or directly by two wooden blocks. As in the previous study [9], the tan δ values were corrected to be tan δ when all logs were supported by extruded polystyrene foam on wooden blocks.

Measurement of moisture contents of log specimens

The average moisture content of four disks (each with a thickness of approximately 40 mm), which were cut from the interior of the log at intervals of 750–1000 mm, was measured using the oven-dry method and was defined as the measured moisture content of the log. Moreover, the heartwood and sapwood parts from one to four disks were cut separately. The average moisture content of each heartwood or sapwood part was measured using the oven-dry method and was defined as the measured heartwood or sapwood moisture content of the log, respectively.

Theory and calculation methods for loss tangent

Setting longitudinal vibration equation of cylinder with consideration to shear stress

The commonly used longitudinal vibration equation proposed by Timoshenko [18] assumes a beam with uniform density. However, to account for the density difference between sapwood and heartwood, which was the primary focus of this study, a more precise vibration equation must be introduced. In research fields unrelated to wood, previous studies have constructed the equation of motion of longitudinal wave propagation and vibration in cylinders and thin-walled cylinders with radial difference in the mechanical properties, and obtained numerical solutions for the resonance frequencies [12–17]. Therefore, this study considered the longitudinal vibration of a cylinder as a simple log model, based on the above-mentioned studies.

Because the tan δ of wood is small, the equation of motion assumes only elastic behavior and does not include a viscous term to obtain a numerical solution for the equation. Subsequently, tan δ is estimated using the strain energy method as described later in this paper.

First, a polar coordinate system for the cylinder is introduced, and vibration in the z direction is assumed with respect to a cylinder with uniform density ρ, where z is the length direction, r is the radial direction, and θ is the circumferential direction. The equation of motion in the z direction can be written as expressed by Eq. 1, based on Fig. 2 [13].

$$\frac{\partial \tau_{rz}}{\partial r} + \frac{1}{r}\tau_{rz} + \frac{1}{r}\frac{\partial \tau_{\theta z}}{\partial \theta} + \frac{\partial \sigma_{zz}}{\sigma z} = \rho \frac{\partial^2 u_z}{\partial t^2}. \tag{1}$$

Because wood is an anisotropic material, the elastic compliance is defined as follows:

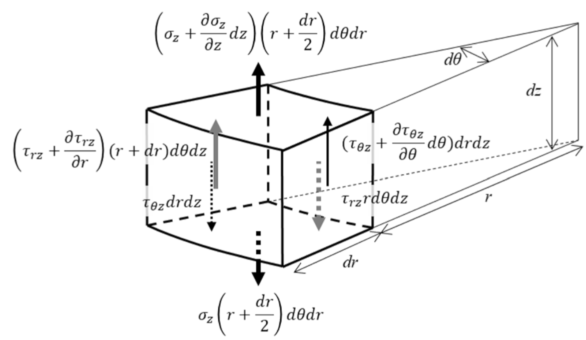

Fig. 2 Forces in z direction acting on volume element in cylindrical coordinates

$$\begin{pmatrix} \sigma_{rr} \\ \sigma_{\theta\theta} \\ \sigma_{zz} \\ \tau_{\theta z} \\ \tau_{zr} \\ \tau_{r\theta} \end{pmatrix} \begin{pmatrix} C_{11} & C_{12} & C_{13} & 0 & 0 & 0 \\ C_{21} & C_{22} & C_{23} & 0 & 0 & 0 \\ C_{31} & C_{32} & C_{33} & 0 & 0 & 0 \\ 0 & 0 & 0 & C_{44} & 0 & 0 \\ 0 & 0 & 0 & 0 & C_{55} & 0 \\ 0 & 0 & 0 & 0 & 0 & C_{66} \end{pmatrix} = \begin{pmatrix} \epsilon_{rr} \\ \epsilon_{\theta\theta} \\ \epsilon_{zz} \\ \epsilon_{\theta z} \\ \epsilon_{zr} \\ \epsilon_{r\theta} \end{pmatrix}.$$

From the equation relating the strain and displacement in the cylindrical coordinate system according to the elastic compliance, Eq. 1 can be rewritten as follows:

$$\begin{aligned} & C_{55}\frac{\partial}{\partial r}\left(\frac{\partial u_r}{\partial z} + \frac{\partial u_z}{\partial r}\right) + C_{55}\frac{1}{r}\left(\frac{\partial u_r}{\partial z} + \frac{\partial u_z}{\partial r}\right) \\ & + C_{44}\frac{1}{r}\frac{\partial}{\partial \theta}\left(\frac{\partial u_z}{r\partial \theta} + \frac{\partial u_\theta}{\partial z}\right) \\ & + \frac{\partial}{\partial z}\left\{C_{31}\frac{\partial u_r}{\partial r} + C_{32}\left(\frac{\partial u_\theta}{r\partial \theta} + \frac{u_r}{r}\right) + C_{33}\frac{\partial u_z}{\partial z}\right\} \\ & = \rho\frac{\partial^2 u_z}{\partial t^2}. \end{aligned} \tag{1$'$}$$

To determine the deformation of logs, it is necessary to compute Eq. 1′. During this calculation, u_θ and the first-order terms of u_r and u_z with respect to θ are ignored, because the motions of u_r and u_z are symmetric about the z axis and independent with respect to the θ direction [13, 14]. Additionally, u_r is considered sufficiently small and can be ignored because wood is an anisotropic material; C_{31} and C_{32} are approximately 0.1 times C_{33}. Additionally, Morino et al. [17] ignored u_r and considered only the z direction in their calculations, and obtained results that were in close agreement with the exact solution when the cylinder model was sufficiently long for their diameter. Hence, Eq. 1′ can be rewritten as follows:

$$C_{55}\left(\frac{\partial^2 u_z}{\partial r^2} + \frac{1}{r}\frac{\partial u_z}{\partial r}\right) + C_{33}\frac{\partial^2 u_z}{\partial z^2} = \rho\frac{\partial^2 u_z}{\partial t^2}. \tag{1$''$}$$

Notably, C_{33} is approximately equal to Young's modulus E in the z direction of wood and C_{55} is the shear modulus G in the z direction on the r-plane. Normally, in the general differential equation for longitudinal vibration proposed by Timoshenko [18], the first term of the left side is also ignored.

Calculation of longitudinal vibration equation of cylinder model with density step

To represent the logs, a cylindrical model considering different densities for the sapwood and heartwood was used. According to previous studies [19–21], in the range of frequencies resulting from the vibration produced by striking the logs, both the wood and the water inside the wood vibrate in the same phase, and the moisture content of the wood can be considered as part of the apparent wood density. Therefore, as expressed by Fig. 3, area ρ_0 was modeled as the sapwood, and area ρ_1 was modeled as the heartwood, with the radius $0<r<r_1$ density as ρ_1, radius $r_1<r<r_0$ density as ρ_0, and average density as ρ_A. Notably, most of the time $\rho_0>\rho_1$, because the moisture content is generally much higher in sapwood. The moisture distribution inside logs other than the sapwood and heartwood was ignored. Although the logs are actually conical in shape, the radius was assumed to be constant in the length direction for simplicity. Moreover, the model's mechanical properties, such as the elastic compliance and axial and shear tan δ, were considered to be constant for simplicity, though actual logs have radial and longitudinal variations in the mechanical properties resulting from the log's growth process [22, 23]. Additionally, E and tan δ of wood are independent of the moisture content in the range above fiber saturation point (FSP) [24], and the moisture content of logs is typically above FSP.

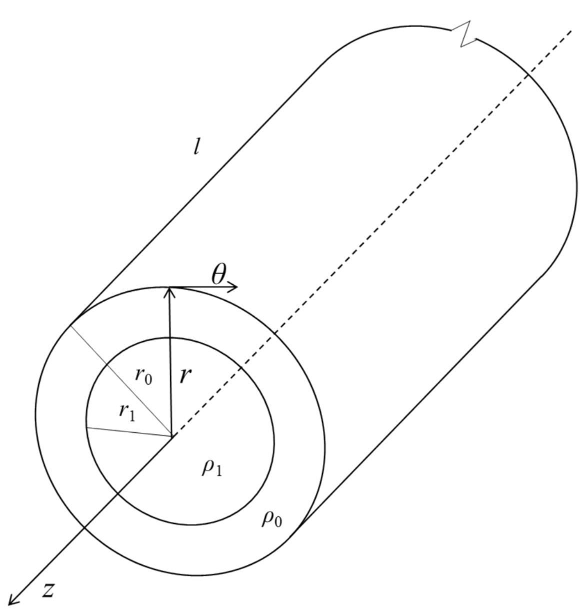

Fig. 3 Cylindrical coordinates of wood log model

Under the above assumptions, the equation of motion in the longitudinal vibration of the model is expressed by Eq. 2, where $r>0$. Hereafter, u_z which means the displacement in the z direction will be referred to as u.

$$\begin{cases} G\left(\frac{\partial^2 u}{\partial r^2}+\frac{1}{r}\frac{\partial u}{\partial r}\right)+E\frac{\partial^2 u}{\partial z^2}=\rho_1\frac{\partial^2 u}{\partial t^2}\ (0<r\le r_1) \\ G\left(\frac{\partial^2 u}{\partial r^2}+\frac{1}{r}\frac{\partial u}{\partial r}\right)+E\frac{\partial^2 u}{\partial z^2}=\rho_0\frac{\partial^2 u}{\partial t^2}\ (r_1<r\le r_0) \end{cases}. \quad (2)$$

Under vibration, because the logs do not separate at the interface of r_1 and move in a body, u can be described as a single function with the same frequency in the z direction. Therefore, while the second term on the left side is the same in the two equations expressed by Eq. 2, the right side is different owing to the different densities. Hence, the first term on the left side, that is, the shear term, should change according to the change on the right side.

Assuming a free–free beam, there is neither shear nor axial stress on the beam surface, and the boundary conditions are expressed as follows:

$$\begin{cases} \tau_{zr}=0(r=0,r_0) \\ \sigma_z=0(z=0,l) \end{cases}. \quad (3)$$

Hereafter, Eq. 2 can be solved by separating variables, where u is expressed as follows:

$$u=X(r)P(z)Q(t). \quad (4)$$

Equation 2 can be transformed into Eq. 2′ using Eq. 4, where $\ddot{X}$ denotes the second derivative of X with respect to r, $\ddot{P}$ with respect to z, and $\ddot{Q}$ with respect to t.

$$\frac{G}{\rho_m}\left(\ddot{X}+\frac{\dot{X}}{r}\right)\frac{1}{X}+\frac{E}{\rho_m}\frac{\ddot{P}}{P}=\frac{\ddot{Q}}{Q}, \quad (2')$$

$$\text{where } m=\begin{cases} 0\,(0<r\le r_1) \\ 1\,(r_1<r\le r_0) \end{cases}.$$

Here, because the cylindrical model representing the logs is excited by longitudinal vibration in the z direction, P (z) and Q (t), for example, can be described as follows:

$$\begin{cases} P(z)=D_1 sinkz+D_2 coskz \\ Q(t)=D_3 sin\omega t+D_4 cos\omega t \end{cases}. \quad (5)$$

These expressions are same as the normal solution of the vibrational equation, where $\ddot{P}/P=-k^2$, $\ddot{Q}/Q=-\omega^2$. Because only the primary mode was considered in this study, $D_1=0$ and $k=\pi/l$ can be calculated from the boundary condition in Eq. 3. Hence, u can be rewritten as follows:

$$u(r,z,t) = X(r)\cos\frac{\pi}{l}z\,\sin(\omega t+\phi). \tag{4'}$$

Let us assume that $\tau=0$; then, the first term on the left side of Eq. 2′ is zero, and the angular frequency ω can be expressed as

$$\omega = \sqrt{\frac{E}{\rho_A}}k = \sqrt{\frac{E}{\rho_A}}\frac{\pi}{l}, \tag{6}$$

using the averaged density ρ_A.

As can be seen, when the cylinder is sufficiently long compared with its diameter, there is little change in the frequency owing to $X(r)$ [13]. In actual measurements, the E/ρ which is calculated from each resonance frequency are almost identical in terms of flexural and longitudinal vibration. Therefore, the resonance frequency is not changed by the shear stress.

By substituting Eq. 6 into Eq. 2′, the following relationship is obtained:

$$\frac{G}{\rho_m}\left(\ddot{X}+\frac{\dot{X}}{r}\right)\frac{1}{X} = E\left(\frac{1}{\rho_m}-\frac{1}{\rho_A}\right)\frac{\pi^2}{l^2}. \tag{7}$$

Further rearrangement yields the following relationship:

$$\frac{\partial^2 X}{\partial r^2}+\frac{1}{r}\frac{\partial X}{\partial r}-\frac{E}{G}\left(\frac{\rho_A-\rho_m}{\rho_A}\right)\frac{\pi^2}{l^2}X = 0. \tag{7'}$$

By applying the boundary conditions of Eq. 3 and solving Eq. 7′, the solution of $X(r)$ is obtained, which clarifies the displacement of longitudinal vibration including radial deformation.

Calculation of tan *δ* using strain energy from axial and shear stress

The objective of this study was to calculate how much tan δ from longitudinal vibration changes owing to the inhomogeneous density inside the logs. However, the displacement function u discussed in the previous section does not include a damping element. Therefore, based on previous studies [25–27] that evaluated the damping by considering the strain energy, this study estimated the effect of inhomogeneous density on tan δ in the longitudinal vibration of logs from the respective strain energy derived from both the axial and shear stress, and the tan δ associated with each stress.

Because both the axial and shear stress change in the same frequency as that in Eq. 4′, the maximum strain energy, which is independent of the time domain, can be used to compare the strain energy. Let the maximum axial strain energy be U_{Amax} and the maximum shear strain energy be U_{Smax}; then, the entire strain energy in the cylinder model can be described as follows:

$$\begin{cases} U_{\mathrm{Amax}} = \frac{1}{2}\iiint \frac{\sigma_z^2}{E} r dr d\theta dz \\ U_{\mathrm{Smax}} = \frac{1}{2}\iiint \frac{\tau_{zr}^2}{G} r dr d\theta dz \end{cases}. \tag{8}$$

From Eq. 4, σ_z and τ_{zr} can be described as follows:

$$\begin{cases} \sigma_z = \frac{\partial u}{\partial z} = X\overline{Q}\frac{\partial P}{\partial z} = X\overline{Q}\left(-\frac{\pi}{l}D_2\sin\frac{\pi}{l}z\right) \\ \tau_{zr} = \frac{\partial u}{\partial r} = P\overline{Q}\frac{\partial X}{\partial r} = \frac{\partial X}{\partial r}\overline{Q}D_2\cos\frac{\pi}{l}z \end{cases}, \tag{9}$$

where $\overline{Q}$ is the maximum amplitude of Q.

Introducing D_5 as constant value and substituting Eq. 9 into Eq. 8 yields the following relationships:

$$\begin{cases} U_{\mathrm{Amax}} = \frac{D_5}{2E}\iint X^2 r dr d\theta \int \left(-\frac{\pi}{l}D_2\sin\frac{\pi}{l}z\right)^2 dz \\ U_{\mathrm{Smax}} = \frac{D_5}{2G}\iint \left(\frac{\partial X}{\partial r}\right)^2 r dr d\theta \int \left(D_2\cos\frac{\pi}{l}z\right)^2 dz \end{cases} \tag{10}$$

Moreover, by introducing a new constant value D_6, Eq. 10 can be rewritten as follows:

$$\begin{cases} U_{\mathrm{Amax}} = D_6\frac{\pi^2}{l^2}\int X^2 r dr \\ U_{\mathrm{Smax}} = D_6\frac{E}{G}\int \left(\frac{\partial X}{\partial r}\right)^2 r dr \end{cases}. \tag{10'}$$

Hence, U_{Amax} and U_{Smax} can be calculated based on $X(r)$.

Moreover, the tan δ measured from the longitudinal vibration can be described as Eq. 11 using tan δ_A, which is derived from axial deformation, and tan δ_S, which is derived from the shear deformation of the longitudinal vibration.

$$\tan\delta = \frac{U_{\mathrm{Amax}}}{U_{\mathrm{Amax}}+U_{\mathrm{Smax}}}\tan\delta_A + \frac{U_{\mathrm{Smax}}}{U_{\mathrm{Amax}}+U_{\mathrm{Smax}}}\tan\delta_S. \tag{11}$$

Hereafter, the rate of increase of tan δ in the longitudinal vibration H is defined as the ratio of tan δ in the longitudinal vibration to the tan δ derived from the axial deformation, tan δ_A. Therefore, using Eq. 11, H can be expressed as follows:

$$H = \frac{\tan\delta}{\tan\delta_A} = \frac{U_{\mathrm{Amax}}}{U_{\mathrm{Amax}}+U_{\mathrm{Smax}}} + \frac{U_{\mathrm{Smax}}}{U_{\mathrm{Amax}}+U_{\mathrm{Smax}}}\frac{\tan\delta_S}{\tan\delta_A}. \tag{12}$$

Numerical conditions

To calculate H from Equations 7′, 10′, and 12, the values of ρ_0/ρ_1, E/G, and tan δ_S/tan δ_A, and the dimensions of r_0, r_1, and l, must be obtained. Based on the actual measurement of log specimens, $r_0/r_1 = 0.68$ and $l/r_0 = 33.4$ are used as the dimension conditions. Notably, E/G and tan

δ_S/tan δ_A were not measured from the logs. Therefore, in this study, the sugi logs' E/G and tan δ_S/tan δ_A values above the FSP were estimated based on several previous papers. The values were determined by considering that the average E of the log specimens used in this study was approximately 10 GPa.

First, regarding E/G, because the direct measurement of the shear modulus of logs has not been reported, the shear moduli in the LR direction obtained in previous studies for small specimens and square timbers were used. Yamai [28] calculated $E/G=13.4$ by carrying out compression tests on small specimens and using the Jenkin formula. Sobue et al. [29] measured E/G of sugi boxed heart squared sawn timber after air seasoning and determined E/G as approximately 15 when E was 10 GPa. Moreover, some studies [30, 31] have reported that the E/G of wood above the FSP is larger than that of air-dried wood, and the ratio is approximately 1.2. Ueda et al. [32] demonstrated that the shear modulus G of commercial sugi boxed-hearted lumbers in the green condition is approximately half of that of the same lumbers after drying. Because it is well known that E above the FSP is approximately 0.8 times that of the air-dried condition [33], E/G in the green condition may be at most 1.6 times that of the air-dried condition. Hence, E/G of the logs is assumed to be 15–25 in this study.

Regarding tan δ_S/tan δ_A, its measurement from logs has not been reported. Obataya [31] obtained the value of approximately 3 in the condition of above the FSP from the small specimens of some species including sugi. Ono [34] also obtained the value of 2–3.5 from small air-dried specimens of several species. Additionally, tan δ_S/tan δ_A is considered to increase exponentially with E/G. From the experimental equations obtained from 101 tree species in air-dried condition [35, 36], tan δ_S/tan $\delta_A=2.5$ when $E/G=15$ and tan δ_S/tan $\delta_A=3.8$ when $E/G=20$. Hence, the tan δ_S/tan δ_A of logs is assumed to be 3–4 in this study.

Results and discussion

Vibrational properties measured from logs

Figure 4 shows the relationship of E/ρ and tan δ for flexural and longitudinal vibration, as measured from log specimens. The tan δ values for the flexural and longitudinal vibration are poorly correlated, while the E/ρ values approximately coincide with each other. This difference is attributed to the particular log characteristics, because previous studies [37, 38] using small clear specimens have reported that there is little difference in tan δ between flexural and longitudinal vibration. Notably, heartwood and sapwood of logs vibrate in a completely identical manner, because the same resonance frequency and tan δ are obtained regardless of whether the sapwood or heartwood are stricken by a hammer or have a piezoelectric acceleration sensor attached to them.

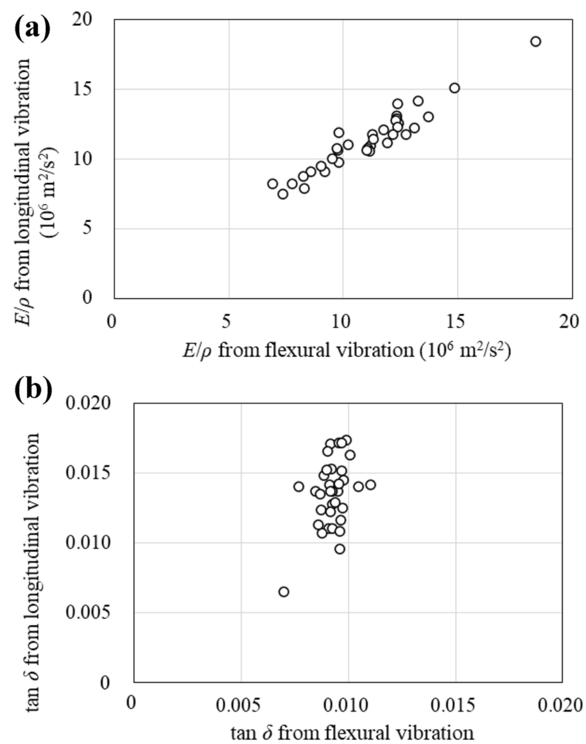

Fig. 4 Relationships of E/ρ and tan δ under flexural and longitudinal vibration: **a** E/ρ; **b** tan δ

Moreover, when the average moisture contents of the logs are corrected to be same, there is negative correlation between E/ρ and tan δ for flexural vibration, which is well known for small clear specimens [39]. However, there is no correlation between E/ρ and tan δ for longitudinal vibration. Therefore, it is considered that tan δ for longitudinal vibration increases owing to a certain factor, while tan δ for flexural vibration exhibits the average tan δ value inside the logs. In this study, the shear deformation in flexural vibration was ignored because the log diameter was small compared with the beam length [18, 40–42].

The average sapwood moisture content was 163% (range of 87%–228%), and the average heartwood moisture content was 91% (range of 53%–178%) for all log specimens. The average sapwood density in green condition was 983 kg/m^3 (range of 716–1265 kg/m^3) and that of heartwood was 738 kg/m^3 (range of 577–1023 kg/m^3). Some logs with low sapwood moisture content had already lost some of their bark and appeared to start to dry.

Figure 5 shows the relationship between the ratio of the apparent sapwood density to that of heartwood, which was calculated from the moisture content difference, and

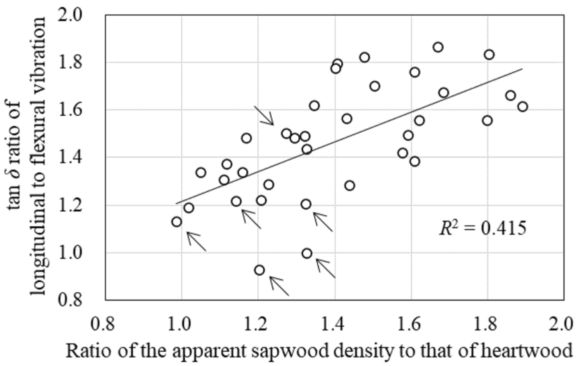

Fig. 5 Relationship between the ratio of apparent sapwood density to that of heartwood and ratio of loss tangent from longitudinal vibration to that from flexural vibration. Arrows indicate the logs whose sapwood moisture content is below 120%

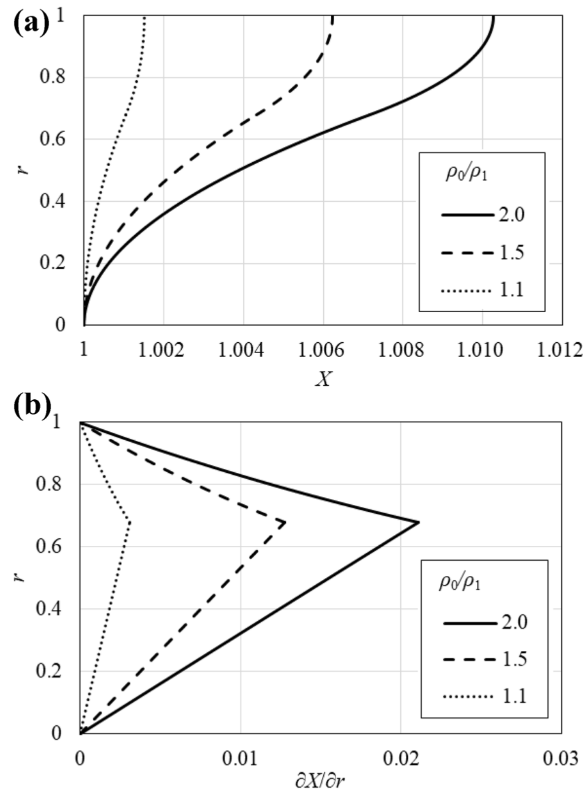

Fig. 6 Calculation results for $X(r)$: **a** X; **b** $\partial X/\partial r$. For better clarity, r is placed on the vertical axis

the tan δ ratio of the longitudinal to the flexural vibration so as to verify the cause for the increase in tan δ under longitudinal vibration. In this study, the oven-dry density was assumed to be same in the radial direction, because the averaged sapwood to heartwood oven-dry density ratio was 0.98 (with standard deviation 0.05) for all log specimens. This is consistent with the study by Ishiguri et al. [43], who reported that the air-dry density of sugi was approximately stable or slightly lower toward the bark in the radial direction. In Fig. 5, the tan δ from longitudinal vibration increases with the ratio of apparent sapwood density to that of heartwood, despite some variations. Therefore, the increase in tan δ from the longitudinal vibration is attributed to the apparent density difference caused by the moisture content difference between the sapwood and the heartwood.

Calculation results for rate of increase of tan δ obtained by numerical solution of longitudinal vibration

First, the longitudinal vibration equation of the cylindrical model with a density difference was calculated. Although Eq. 7′ can be calculated using the Bessel function [13–17], this study obtained a numerical solution using the Euler method for simplicity. Figure 6 shows the calculation results for X and $\partial X/\partial r$ in the range of $0<r\leq 1$, with $X=1$ and $\partial X/\partial r=0$ at $r=0.001$ and $r_0=1$ as the initial value, and with X being continuous and differentiable at $r=r_1$ and the calculation interval $\Delta r=0.001$ as the calculation condition; $r_1=0.68$ and $l=33.4$ are the measured values of the log specimens; $E/G=20$; $\rho_0/\rho_1=1.1$, 1.5, or 2.0.

Subsequently, both the axial and shear strain energy can be calculated using Eq. 10′. Figure 7 shows the calculation results for U_{Amax} and U_{Smax} as ratios to U, which is the maximum axial strain energy when there is no density difference, with respect to the apparent density ratio when $E/G=15$, 20, or 25. The X value is particularly large at $r_1/r_0=0.68$ because the cross-sectional area of the sapwood and heartwood is approximately the same.

Finally, the rate of increase of tan δ in the longitudinal vibration H can be calculated using Eq. 12. Figure 8 shows the calculation results for H using tan δ_{S}/tan $\delta_{\mathrm{A}}=3$ or 4. As E/G and tan δ_{S}/tan δ_{A} increase, the more tan δ from the longitudinal vibration increases with the

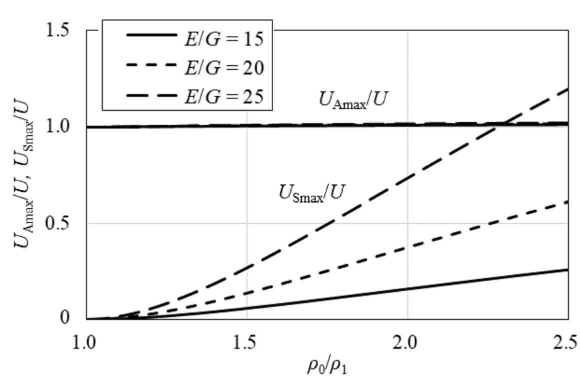

Fig. 7 Change in U_{Amax} and U_{Smax} by increase in ρ_0/ρ_1

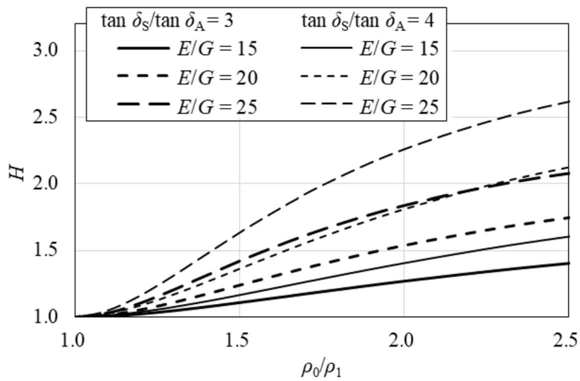

Fig. 8 Change in H by increase in ρ_0/ρ_1 under various mechanical properties

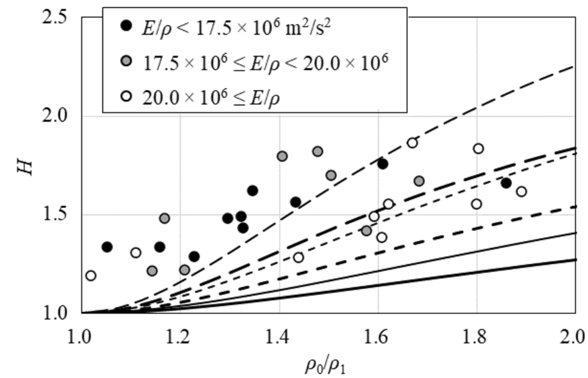

Fig. 9 Comparison between measured H from sugi logs and calculated H. Difference in color denotes the classification of logs by corrected E/ρ in their moisture contents at FSP. The six lines are the same as Fig. 8. The logs whose sapwood moisture content is below 120% are excluded

sapwood to heartwood density ratio. When the sapwood to heartwood density ratio is 2, H, the rate of increase of tan δ is calculated in the range of 1.3–2.3.

Comparison between measured and calculated rate of increase of tan δ for longitudinal vibration owing to apparent density difference

First, measured H was defined for comparison to calculated H. Under flexural vibration, the density variation in the radial direction affects only the rotary inertia [18], in contrast to the vibrational properties, which are affected more by the surface rather than by the core according to the moment of inertia of the area. However, the effect of rotary inertia is small for the primary mode of a beam with sufficient length relative to the height [18]. Moreover, as discussed in the previous section, the shear modulus concerning the flexural vibration with a sufficient log length can be ignored [40–42]. Therefore, this study assumed the tan δ from flexural vibration as the tan δ from the pure axial stress, tan δ_A, which means that the tan δ ratio of the longitudinal to flexural vibration can be considered as H (measured H).

Figure 9 shows the comparison of the measured H in Fig. 5 to the calculated H in Fig. 8. The calculated H and the measured H exhibit similar increasing trends, particularly with high ρ_0/ρ_1. Hence, it is concluded that the increase of the tan δ from longitudinal vibration compared with that from flexural vibration may have been caused by shear stress occurring around the sapwood and heartwood interface, owing to the apparent density difference.

However, as shown in Fig. 9, the measured H tended to be larger than the calculated H overall. Particularly, even when there was no difference in the apparent densities of the sapwood and heartwood, the longitudinal vibration tan δ was at least 1.2 times higher than that of the flexural vibration, except for logs that appeared to start to dry. For logs with no disparity in the sapwood and heartwood moisture content, and logs that have not yet started drying, both the sapwood and heartwood maintain high moisture content levels. This suggests that, even if the measured sapwood and heartwood moisture content appear similar, there could be non-uniform moisture distribution within both, including localized drops in moisture content, particularly in the transition zone. Although detailed moisture content distribution was not measured in this study, Nakada [11] indicated that heartwood moisture content sometimes varies a lot. Consequently, the actual radial density distribution is likely more intricate than assumed in this study, giving rise to complex shear stresses in the model. This is consistent with the fact that the measured H values are lower for some logs with low sapwood moisture content that exhibit the initiation of drying (as indicated by the arrows in Fig. 5).

Moreover, by classifying the logs by E/ρ and adjusting their moisture content to be the FSP, it was found that smaller E/ρ values tend to have larger H within the same ρ_0/ρ_1 ratio. Considering that previous research [44] has shown that timber with knots has smaller E and larger E/G compared with timber without knots, it follows that logs with smaller E and larger E/G exhibit larger increase in tan δ, although the variation reported by a previous study is too large.

Conclusions

This study clarified that, as the ratio of apparent sapwood density to that of heartwood increases owing to the difference in moisture content, the tan δ for longitudinal vibration increases compared with that for flexural vibration. Additionally, it was shown the increase of tan δ can be explained by the shear modulus induced inside the log when the sapwood and heartwood have different apparent densities. By comparing the vibrational properties of the longitudinal and flexural vibrations of 35 sugi logs, it was found that tan δ differed significantly, while E/ρ was approximately the same. Positive correlation was observed between the ratio of apparent sapwood density to that of heartwood, and the ratio of tan δ of longitudinal vibration to flexural vibration. Then, to calculate tan δ, a cylindrical model considering the apparent density difference of sapwood and heartwood was introduced. By calculating the axial and shear strain energy through the numerical solution of a differential equation, it was found that the shear strain energy increases in accordance with the density difference ratio. The rate of increase of tan δ calculated based on literature data is in good agreement with the measured rate of increase of tan δ under longitudinal vibration.

Abbreviation

FSP Fiber saturation point

Acknowledgements

The corresponding author would like to thank Dr. Daisuke Kono, associate professor of Kyoto University, graduate school of engineering, division of micro engineering, and Dr. Kotaro Mori, program-specific assistant professor of Kyoto University, graduate school of engineering, and division of micro engineering, for useful discussions and comments for the calculation of longitudinal vibration model.

Author contributions

TF contributed to the conceptualization, investigation, methodology, visualization, and original draft of the manuscript. YY contributed to the data curation, formal analysis, investigation, methodology, and review and editing of the manuscript. YF contributed to the conceptualization, data curation, funding acquisition, investigation, methodology, project administration, supervision, validation, visualization, and review and editing of the manuscript. All the authors have read and approved the final manuscript.

Funding

This work was performed as part of a research project funded by Kyoto University.

Availability of data and materials

The datasets used and/or analyzed during this study are available upon request from the corresponding author.

Declarations

Competing interests

The authors declare that they have no competing interests.

Received: 27 September 2023 Accepted: 19 November 2023
Published online: 08 December 2023

References

1. Oja J, Grundberg S, Grönlund A (2001) Predicting the stiffness of sawn products by X-ray scanning of Norway spruce saw logs. Scand J For Res 16:88–96
2. Ikeda K, Nagase W, Sugiyama A, Miyoshi Y, Suzuki Y (2021) Development of methods for estimating the moisture content of large-diameter sugi (*Cryptomeria japonica*) logs using gamma rays and high-frequency electromagnetic waves (in Japanese). Mokuzai Kogyo 76:444–449
3. Suzuki Y, Ikeda K, Miyoshi Y, Fujimoto K, Sugiyama A (2018) Evaluation of moisture content of sugi logs using impedance measurement. 2018 12th ISEMA, Lublin, Poland, pp 1–3, https://doi.org/10.1109/ISEMA.2018.8442300
4. Wang X, Ross RJ, McClellan M, Barbour RJ, Erikson JR, Forsman JW, McGinnis GD (2001) Nondestructive evaluation of standing trees with a stress wave method. Wood Fiber Sci 33:522–533
5. Shiiba A, Aratake S, Morita H (2011) Mechanical performance of sugi (*Cryptomeria japonica*) lumber sawn parallel to the edge of large diameter logs I (in Japanese). Mokuzai Gakkaishi 57:234–241
6. Ross RJ, McDonald KA, Green DW, Schad KC (1997) Relationship between log and lumber modulus of elasticity. For Prod J 47:89–92
7. Ross RJ (2015) Nondestructive evaluation of wood: second edition. USDA Forest service, FPL-GTR-238. Madison
8. Fukui T, Yanase Y, Sawada Y, Fujii Y (2020) Estimations of the moisture content above the fiber saturation point in sugi wood using the correlation between the specific dynamic Young's modulus and tangent loss. J Wood Sci 66:35 https://doi.org/10.1186/s10086-020-01879-y
9. Fukui T, Yanase Y, Fujii Y (2023) Moisture content estimation of green softwood logs of three species based on measurements of flexural vibration. J Wood Sci. 69:32 https://doi.org/10.1186/s10086-023-02106-0
10. Nakada R, Fujisawa Y, Hirakawa Y (1999) Soft X-ray observation of water distribution in the stem of *Cryptomeria japonica* D. Don II: types found in wet-area distribution patterns in transverse sections of the stem. J Wood Sci 45:194–199
11. Nakada R (2007) Variation of water distribution within living stems and its casual factors in *Criptomeria Japonica* (L. f.) D. Don (in Japanese). Bull For Breed Center 23:121–254
12. Gazis DC (1959) Three-dimensional investigation of the propagation of waves in hollow circular cylinders. I J Acoust Soc Am 31:568–573
13. Kolsky H (1963) Stress waves in solids. Dover Publications, New York
14. McNiven HD, Sackman JL, Shah AH (1963) Dispersion of axially symmetric waves in composite, elastic rods. J Acoust Soc Am 35:1602–1609
15. Rumerman M, Raynor S (1971) Natural frequencies of finite circular cylinders in axially symmetric longitudinal vibration. J Sound Vib 15:529–543
16. Nelson RB, Dong SB, Kalra RD (1971) Vibrations and waves in laminated orthotropic circular cylinders. J Sound Vib 18:429–444
17. Morino Y, Mori D (1976) On the longitudinal shock and vibration of cylindrical solid rocket motor cases (in Japanese). Aeronaut Space Sci Jpn 24:542–552
18. Timoshenko S (1955) Vibration problems in engineering. Van Nostrand, New York
19. Gerhards CC (1975) Stress wave speed and MOE of sweetgum ranging from 150 to 15 percent MC. For Prod J 25:51–57
20. James WL, Boone RS, Galligan WL (1982) Using speed of sound in wood to monitor drying in a kiln. For Prod J 32:27–34
21. Sobue N (1993) Simulation study on stress wave velocity in wood above fiber saturation point (in Japanese). Mokuzai Gakkaishi 39:271–276
22. Nakada R, Fujisawa Y, Hirakawa Y (2003) Effects of clonal selection by microfibril angle on the genetic improvement of stiffness in *Cryptomeria japonica* D. Don Holzforschung 57:553–560
23. Nakada R, Fujisawa Y, Hirakawa Y, Yamashita K (1998) Longitudinal change of the green moisture content in the stem of *Cryptomeria japonica* D. Don (in Japanese). Mokuzai Gakkaishi 44:395–402
24. Kollmann F, Krech H (1960) Dynamic measurement of damping capacity and elastic properties of wood. Holz Roh Werkst 18:41–54
25. Lin DX, Ni RG, Adams RD (1984) Prediction and measurement of the vibrational damping parameters of carbon and glass fibre-reinforced plastics plates. J Compos Mater 18:132–152
26. Adams RD, Maheri MR (1994) Dynamic flexural properties of anisotropic fibrous composite beams. Compos Sci Technol 50:497–514
27. Berthelot JM (2006) Damping analysis of laminated beams and plates using the Ritz method. Compos Struct 74:186–201
28. Yamai R (1959) Studies on the orthotropic properties of wood in compression (in Japanese). Bull Gov Forest Exp Station 113:57–112
29. Sobue N, Ikeda K (1999) Torsional vibration test of sugi boxed heart squared sawn timber (in Japanese). Mokuzai Gakkaishi 45:289–296

30. Gerhards CC (1982) Effect of moisture content and temperature on the mechanical properties of wood: an analysis of immediate effects. Wood Fib Sci 14:4–36
31. Obataya E (1999) Suitability of acetylated woods for clarinet reed. J Wood Sci 45:106–112
32. Ueda Y, Shibata H, Kuramoto K, Morita H (2012) Ascending in static modulus of transverse elasticity on high-temperature drying (in Japanese). Bull Tottori Pref Forest Exp Station 44:51–55
33. Brémaud I, Gril J (2021) Moisture content dependence of anisotropic vibrational properties of wood at quasi equilibrium: analytical review and multi-trajectories experiments. Holzforschung 75:313–327
34. Ono T (1980) The dynamic rigidity modulus and internal friction of several woods in torsional vibration. Mokuzai Gakkaishi 26:139–145
35. Aizawa H, Obataya E, Ono T, Norimoto M (1998) Acoustic converting efficiency and anisotropic nature of wood. Wood Res 85:81–83
36. Obataya E, Ono T, Norimoto M (2000) Vibrational properties of wood along the grain. J Mater Sci 35:2993–3001
37. Tonosaki M, Okano T, Asano I (1983) Vibrational properties of Sitka Spruce with longitudinal vibration and flexural vibration (in Japanese). Mokuzai Gakkaishi 29:547–552
38. Brancheriau L, Kouchade C, Brémaud I (2010) Internal friction measurement of tropical species by various acoustic methods. J Wood Sci 56:371–379
39. Ono T, Norimoto M (1984) On physical criteria for the selection of wood for soundboards of musical instruments. Rheol Acta 23:652–656
40. Yoshihara H, Yoshinobu M (2015) Young's modulus and shear modulus of solid wood measured by the flexural vibration test of specimens with large height/length ratios. Holzforschung 69:493–499
41. Nakao T, Okano T, Asano I (1985) Theoretical and experimental analysis of flexural vibration of the viscoelastic Timoshenko beam. J Appl Mech 52:728–731
42. Divos F, Tanaka T, Nagao H, Kato H (1998) Determination of shear modulus on construction size timber. Wood Sci Technol 32:393–402
43. Ishiguri F, Terazawa E, Sanpe H, Matsumoto K, Ishidoh M, Ohono H, Iizuka K, Yokota S, Yoshizawa N (2009) Radial variation and difference between juvenile wood and mature wood in bending property of sugi (*Criptomeria Japonica* D. Don) originated from seedlings (in Japanese). Mokuzai Kogyo 64:20–25
44. Chui YH (1991) Simultaneous evaluation of bending and shear moduli of wood and the influence of knots on these parameters. Wood Sci Technol 25:125–134

Publisher's Note